NATO Undersea Research Centre
Centre de Recherche Sous-Marine de l'OTAN

Reprint Series **NURC-PR-2006-008**

Contact-Level Multistatic Sonar Data Simulator for Tracker Performance Assessment

Grimmett Doug, Coraluppi Stefano

August 2006

Originally published in:

FUSION 2006, The 9th International Conference on Information Fusion 2006, Florence (Italy), 10-13 July 2006, Conference Proceedings.

NATO Undersea Research Centre (NURC)

NURC conducts world class maritime research in support of NATO's operational and transformational requirements. Reporting to the Supreme Allied Commander Transformation, the Centre maintains extensive partnering to expand its research output, promote maritime innovation and foster more rapid implementation of research products.

The Scientific Programme of Work (SPOW) is the core of the Centre's activities and is organized into four Research Thrust Areas:

- Expeditionary Mine Countermeasures (MCM) and Port Protection (EMP)
- Reconnaissance, Surveillance and Undersea Networks (RSN)
- Expeditionary Operations Support (EOS)
- Command and Operational Support (COS)

NURC also provides services to other sponsors through the Supplementary Work Program (SWP). These activities are undertaken to accelerate implementation of new military capabilities for NATO and the Nations, to provide assistance to the Nations, and to ensure that the Centre's maritime capabilities are sustained in a fully productive and economic manner. Examples of supplementary work include ship chartering, military experimentation, collaborative work with or services to Nations and industry.

NURC's plans and operations are extensively and regularly reviewed by outside bodies including peer review of the research, independent national expert oversight, review of proposed deliverables by military user authorities, and independent business process certification. The Scientific Committee of National Representatives, membership of which is open to all NATO nations, provides scientific guidance to the Centre and the Supreme Allied Commander Transformation.

NOTE: The NURC Reprint series reprints papers and articles published by NURC authors in the open literature as an effort to widely disseminate NURC products. Users are encouraged to cite the original article where possible.

Contact-Level Multistatic Sonar Data Simulator for Tracker Performance Assessment

Doug Grimmett[1]
NATO Undersea Research Centre (NURC)
Viale S. Bartolomeo 400, 19138 La Spezia, Italy

Stefano Coraluppi
NATO Undersea Research Centre (NURC)
Viale S. Bartolomeo 400, 19138 La Spezia, Italy
coraluppi@nurc.nato.int

Abstract - *This paper provides an overview of a multistatic sonar contact-data simulation approach and a dataset generated specifically for tracker algorithm evaluation by the Multistatic Tracking Working Group (MSTWG). A brief description of the simulation approach is given, which includes simple sonar equation modeling, resulting in sensor-to-sensor target fading effects, as well as contact localization modeling. We describe the methodology by which a single data set generated using this approach is suitable to evaluate multistatic tracker performance over a range of multi-sensor detection redundancy levels.*

Keywords: Multistatic Sonar - Sensor Fusion – Tracker Performance Models - Distributed Tracking – Sonar Performance Modeling and Simulation

1 Introduction

Operationally effective multistatic sonar and radar systems must include robust, automated multi-sensor fusion and target tracking algorithms. This is no small challenge as each of the multistatic network's source-receiver nodes provides a high number of false alarms in addition to target detections. Recent interest in this research area has led to the formation of the Multistatic Tracking Working Group (MSTWG), whose goal is to foster the exchange of scientific and technical ideas, problems, and solutions related to multistatic tracking for sonar and radar. This will include the collaborative analysis of common data sets, with a common set of performance metrics [1].

This paper describes a detection-level, contact-based multistatic active data simulation, provided by the NATO Undersea Research Centre to the working group for tracker evaluation. The modeled dataset is for a mobile multistatic sonar scenario. The approach makes some significant modeling assumptions, while still providing the type of inter-sensor target fading effects seen in real at-sea datasets, with which tracking algorithms must contend.

The simulation capability allows for arbitrary system and measurement errors as described in [2].

2 Simplified Sonar Equation Modeling

Accurate modeling of sonar system performance is non-trivial, given the complexity of the underwater acoustic environment. Even if high fidelity acoustic propagation, reverberation, and noise modeling are attempted, it is usually the case that the model input parameters are not knowable to the degree necessary to make predictive performance estimates for a specific operating area. What is initially required for the multistatic tracker evaluation is not a predictive, high-fidelity model, but one which captures the gross features sonar performance as a function of the geometric placement.

We start by assuming that the sonar network is situated in a reverberation-limited environment, dominated by sea bottom reflections. This assumption simplifies the modeling, but it is also often the case in shallow water environments where sonar systems are currently expected to operate. Of course at long range to the sensors, such an assumption would no longer be valid, and noise-limited modeling would need to be included. The bistatic sonar equation for a reverberation-limited active sonar is given as

$$SE = EL - RL - DT \tag{1}$$

where SE is the signal excess in dB above a detection threshold DT. EL is the target's echo level against a reverberation background level RL, as given by

$$\begin{aligned} EL &= SL - TL_{ST} - TL_{TR} + TS \\ RL &= SL - TL_{SP} - TL_{PR} + BTS \end{aligned} \tag{2}$$

where SL is the transmitter's source level, TL_{ST} and TL_{SP} are the transmission losses from the source to target and the reverberation patch, TL_{TR} and TL_{PR} are the transmission losses from the target and the reverberation patch to the receiver, TS is the target strength, and BTS is the bottom target strength. A bistatic sonar node's source and receiver act as foci to a set of equi-time ellipses, where target echoes may occur at particular time delays (from sonar transmission).

[1] Work performed while at NURC. Current e-mail address: grimmett@spawar.navy.mil.

We assume here, for the purposes of this simplified model, that propagation losses are similar for the target and the ensonified reverberation patch beneath it. This approximation can be justifiably made in many shallow water environments. Making this assumption (i.e., $TL_{ST} = TL_{SP}$, and $TL_{TR} = TL_{TP}$), we obtain

$$SE = TS - BTS - DT \, . \qquad (3)$$

The bistatic TS is normally a target aspect-dependent function, for which models exist. In general it can be assumed that there is a large enhancement in the TS when the angle of target ensonification is equal or close to the same as the reflected angle (around a reference perpendicular to the target's heading). When the target provides a bow or stern aspect it is normally assumed that the TS decreases.

The BTS is the amount of energy seen by the system due to scatterers located on or under the ocean bottom interface. The bistatic BTS can be complicated to determine. In general it is dependent on the bottom scattering strength (itself a function of acoustic grazing angle), the ensonified patch size, and the effects of processing the active received waveform. The bottom scattering strength is a function of the acoustic reflective properties of the bottom material. The ensonified patch size is determined by the range to the receiver, the sonar pulse-length and the elliptical segment subtended by each of the receiver's azimuthal beams. The received reverberation can be further reduced via standard signal processing (matched filtering to the transmitted or Doppler-shifted versions of the sonar waveform).

The modeling may be done for a static geometry of sources and receivers, calculating the SE everywhere over a surrounding grid of potential target locations, assuming a constant target heading. Alternatively, the model may output the SE for each sonar (source-receiver) node over time, assuming mobile trajectories for the sonar sources, receivers and targets. The latter is the mode that is used for the multistatic contact simulation application. A scenario is generated, and the signal excess is calculated for each ping time and node. When DT= 0 dB, the model outputs SNR (SE = SNR). These levels serve as the mean target detection SNRs for the contact simulation. More details about this simplified signal excess modeling approach is given in [3].

3 Mobile Multistatic LFAS Scenario

The scenario under consideration assumes three ships, each equipped with Low Frequency Active Sonar (LFAS) equipment. One ship is assumed to be a monostatic platform, i.e., one which hosts a nearly collocated towed transmitter and towed array receiver. The other two ships provide bistatic capabilities through the provision of an additional transmitter and receiver, respectively. The sonar assets are as follows:

- Ship 1: hosts TX1 and RX2
- Ship 2: hosts TX2
- Ship 3: hosts RX2

The following multistatic detection nodes result:

- TX1 – RX1 (monostatic)
- TX1 – RX2 (bistatic)
- TX2 – RX1 (bistatic)
- TX2 – RX2 (bistatic)

All three ships are heading east, in-line with an inter-ship spacing of 7nm at 5kts. The target trajectory is shown to the north of the assets (in magenta). The target is heading west at 4kts. The geometry of the assets is shown in figure 1, and specified according to the following table.

Table 1. Details of the simulated multistatic geometry.

	Start- X	**Start- Y**	**Heading**	**Speed (kts)**
Ship 1	-14.5	-2.0	East	5
Ship 2	-0.5	-2.2	East	5
Ship 3	-7.5	-1.8	East	5
Target	6.0	5.0	West	4

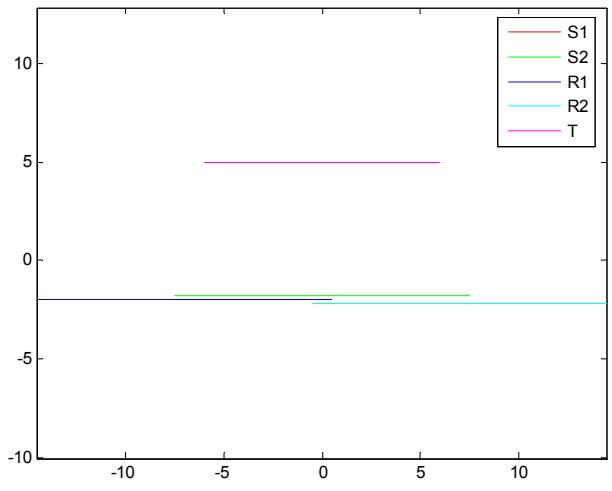

The run scenario duration is 180 minutes, with TX1 and TX2 both transmitting 1-second FM waveforms (300 Hz bandwidth, 2 kHz center frequency) every 60 seconds. CW or other Doppler-sensitive waveforms are not considered here, but will be a focus of future MSTWG tracker evaluation efforts.

4 Target-Contact Simulation

The modeling method described in section 2 was used to model the four different detection nodes for the

scenario described in section 3. We assume a Swerling fluctuation model and a detection threshold of 0dB. Therefore, after each mean SNR is obtained a Rayleigh fluctuation term is added, to give the data more statistical realism. In figure 2, the results of the fluctuating target levels obtained for the four nodes are shown over the scenario's duration (each in a different color). For each ping time (minute) an "x" marks the maximum SNR achieved by any of the four nodes. Here, an offset of +7 dB has been added to the modeled SNR values (leading to the easy version of the scenario, as described for case N1 and N2 in section 6).

The ping-to-ping variability due to the target fluctuation model is clearly seen. In addition, we see that for each node there is a slow varying fading effect on the SNR mean. This is the effect of the changing sensor-target geometry, which is provided by the simple SE model. We see that in the first half of scenario, the best performance is provided by the S1-R2 (green) and S2-R2 (cyan) nodes, while during the second half it is provided by the S1-R1 (red) and S2-R1 (blue) nodes. The effect of the target "specular" condition is evident with the very high values of SNR obtained by the nodes in the time sequence corresponding to when they each experience this "good" look (S2-R2, S1-R2, S2-R1, and S1-R1, respectively).

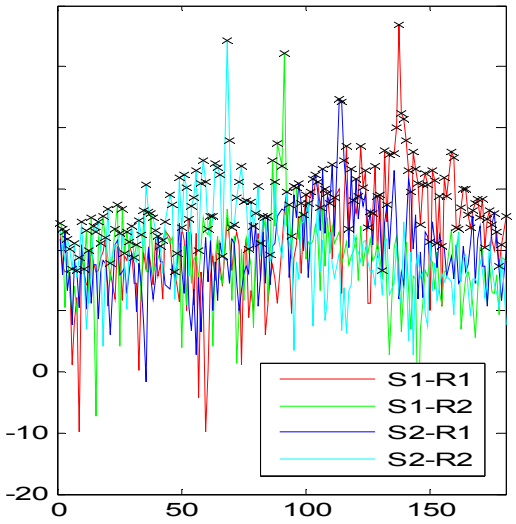

Fig. 2. Mean target SNR for the simulation.

The resulting target SNR contacts for each ping and node are then mapped into the scenario's geometry with localization errors. Localization errors for bistatic systems are determined by various system measurement errors. For this simulation, the following measurement errors (expressed as standard deviations with zero-mean error) were used to determine the offset between the simulated target contact positions and the true target positions:

- Timing errors: 0.01 seconds
- Bearing errors: 2° (random), 1° (bias due to array heading)
- Speed of Sound: 15 m/s (1500 m/s nominal)
- Source/Receiver positional errors: None

The impact of system measurement errors on equivalent measurement covariance matrices is described in [3].

5 False-Contact Simulation

The simulation of false contacts is made with some simplifying assumptions. In shallow water acoustic environments, active sonar systems are faced with large amounts of confusing false alarms (clutter). This clutter is generally generated from clutter returns coming from the intense interaction of the sound on ocean bottom and/or sub-bottom. The statistics of ocean bottom generated clutter are non-Rayleigh. Clutter distributions generally show much higher tails than Rayleigh noise. However, the accurate modeling of such reverberation clutter for sonar is so far not well advanced.

As starting point, and for the purposes of contact simulation for multistatic tracker evaluation, we assume a Raleigh distributed noise background. Another simulation approach is to use collected sea trial data (which does not contain a target) to provide real clutter, and then inject simulated target contacts into the data [4].

For each source-receiver ping, a large number of potential false contacts are generated, by drawing from the Raleigh distribution. The number of draws was chosen to be representative of the number of observation cells in the sonar's measurement space. In this case, we assumed 1.5 million draws corresponding to a sonar with 100 beams, time resolution of 1/300sec, and an acquisition window of 50sec. From these, only the strongest 199 contact SNRs, were selected for each source/receiver/ping contact file. This serves as a simple model of what would be the output of an appropriate normalization/detection/contact-forming processing chain.

Figure 3 illustrates the average false alarm rate (FAR) per contact file as a function of detection threshold in dB. From this we see that with only slight changes in the detection threshold, the FAR changes significantly. This graph will also be important to consider later, if one is interested in raising the detection threshold to limit the number of false alarms for the tracker. Table 2 shows expected FARs as function of detection threshold.

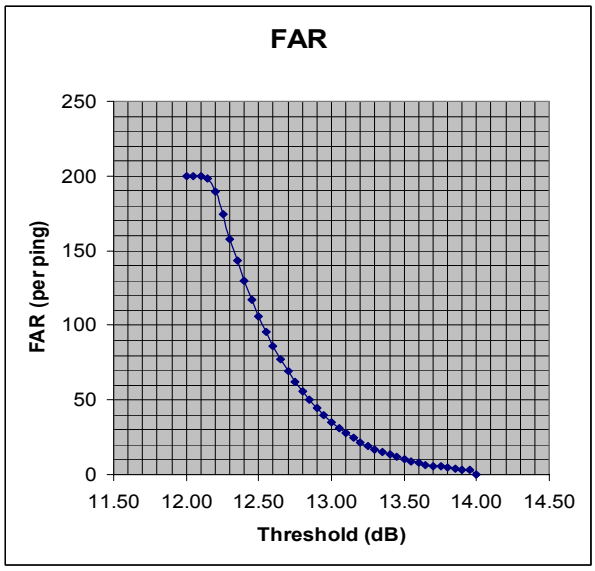

Fig. 3. The average false alarm rate (per ping-node) for the simulated dataset.

Table 2. False alarms rates achieved with different detection thresholds.

FAR (per S-R ping)	Detection Threshold
5	13.75 dB
10	13.5 dB
35	13.0 dB
50	12.85 dB
100	12.5 dB
200	12.0 dB

Using this method, once the false alarm statistics have been generated for each contact file, each false alarm is assigned a geographic location. The locations for the 199 false alarms are then assigned with a uniform distribution in time (delay from waveform reception) and bearing.

6 Scenarios within the Scenario

The primary simulated data set is created by combining the target detection contacts (one per source-receiver node per ping) and the false alarm contacts. This results in 720 files (4 nodes * 180 pings), each with 200 contacts (1 target contact and 199 false contacts).

The simulated scenario is shown in figure 4. False contacts above a threshold of 13.5 dB (corresponding to a nodal false alarm rate of 10 false alarms per ping) are shown in blue for the entire scenario duration. This corresponds to a total of 7200 false alarms (10 * 180 pings *4 nodes). Target contacts are shown in green and receiver trajectories in black. Confirmed output tracks from NURC's multistatic tracker are shown in magenta.

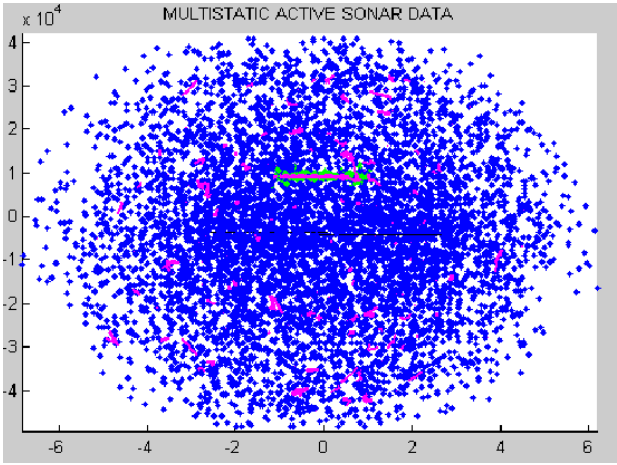

Fig. 4. A geographic plot of simulated target contacts (green) and false contacts (blue).

From the single scenario that has been simulated, we may achieve a number of interesting variants. This is possible to achieve simply, by adjusting the SNR levels of the target contacts and by changing the detection threshold. A summary of various cases that NURC proposes for tracker evaluation in the MSTWG are shown in Table 3.

Particular multistatic tracking algorithms may be well suited to address specific scenarios. Some scenarios will be more challenging than others, depending on the detection performance found in the multistatic network. Also a very critical issue is how well a tracker copes with the increased false alarm rates due to multiple sensors. It is therefore important that the tracker performance be determined over a large set of conditions and scenarios. Some tracking algorithms or architectures may perform well for one scenario, but poorly for another. A robust tracking algorithm will perform relatively well over a large number of scenarios. A characterization of the performance of various tracking algorithms on various scenarios is the envisioned output of the MSTWG. The various scenario variations are now discussed.

Cases N1 and N2 have a high Probability of Detection (PD) on all nodes for most of the run. Therefore these cases have high degree of "detection redundancy" within the multistatic network. These are the baseline cases, as they should be the least challenging for the tracker. These cases are obtained by simply adding 7 dB to all the target contacts (tagged as such within the file format) in the simulated data set. Two different values of false alarm rate are considered (10 for N1 and 35 for N2). Figure 5 show the target detections above the detection threshold for this case for the four nodes. Figure 6 shows the ROC curves for these cases (same color coding as used previously), showing the nodal PD to be about 85%. The cyan curve indicates the improved ROC curve resulting from an optimum fusion of the target detections. Here the fusion rule applied is: the network detects if one or more of four nodes detect the target. In this case the PD improves to 100% for

these scenarios. The effect of FAR variation can be compared between cases N1 and N2.

Table 3. Scenario variants obtainable from dataset.

	PD	FAR /ping, DT (dB)
N1	High PD TGT SNR +7 dB	Low FAR = 10, DT=13.5
N2	High PD TGT SNR +7 dB	High FAR = 35, DT=13.0
N3	Moderate PD TGT SNR +0 dB	Low FAR = 10, DT=13.5
N4	Moderate PD TGT SNR +0 dB	High FAR = 35, DT=13.0
N5	Low PD TGT SNR -7 dB	Low FAR = 10, DT=13.5
N6	Low PD TGT SNR -7 dB	High FAR = 35, DT=13.0
N7	Low PD TGT SNR -7 dB	Variable SNR thresholds as • S1-R1: FAR=0, 14.0 dB • S1-R2: FAR=5, 13.75 dB • S2-R1: FAR=10, 13.5 dB • S2-R2: FAR=35, 13.0 dB
N8	Very low PD as TGT SNR -14dB	Low FAR = 10, DT=13.5

Cases N3 and N4 are more challenging, due to the decreased target SNRs and lower PD levels. Figure 7 shows all target detections above the threshold and figure 8 shows the ROC curve performance. We see that there is much less detection redundancy. For example, we see that the red system does not detect in the first half of the run and the cyan system does not detect in the second half of the run. The ROC curves show that individual nodal PD is around 50%, while the fused case rises to near 90%. These scenarios offer the effects of target fading across the nodes during the run. The same two false alarm rates are considered (10 for N3 and 35 for N4) and results can be compared with cases N1 and N2.

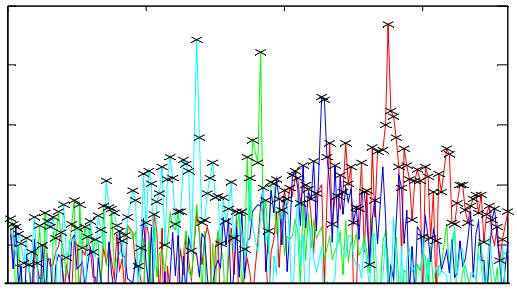

Fig. 5. Target detections above the threshold for cases N1 and N2.

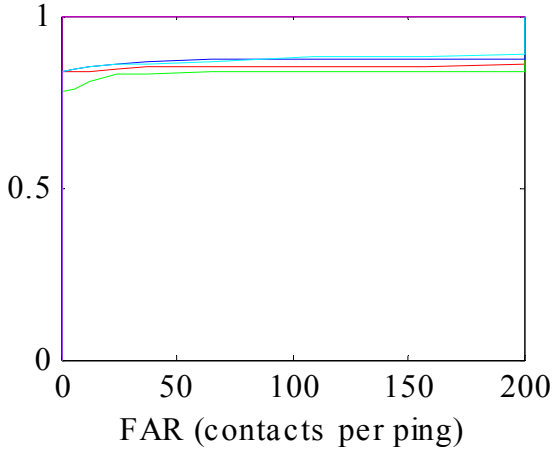

Fig. 6. Individual and fused ROC curve performance for simulated data for cases N1 and N2.

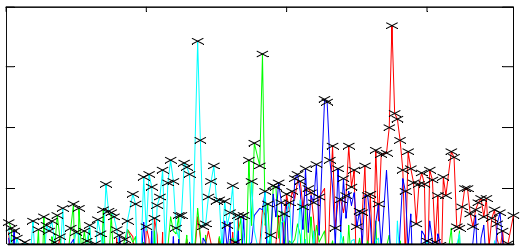

Figure 7. Target detection contacts for cases N3 and N4, with target fading and less detection redundancy.

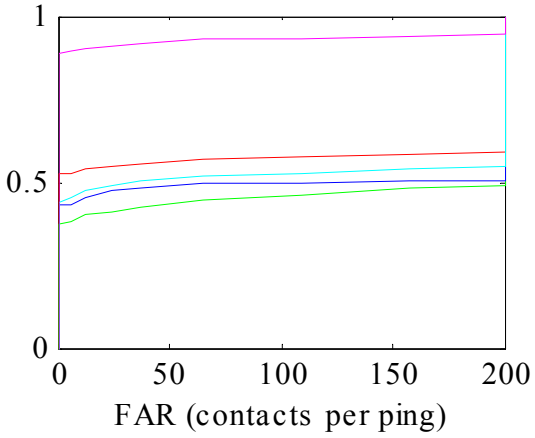

Fig. 8. Individual and fused (cyan) ROC curve performance for cases N3 and N4.

Cases N5 and N6 are obtained by subtracting 7dB from all the target contacts in the simulated data set. These cases are even more challenging, because of the very low level of PD. Figure 9 shows the all target detections above the threshold and figure 10 shows the ROC curve performance. Here we see that the there is virtually no detection redundancy. Each node sees the target and then another nodes subsequently detects. The ROC curves show that individual nodal PD is around 10-25% while the fused case rises only to about 50%. These scenarios offer the conditions where the detection limits of each system are nearly coincident, and the target holding is "handed off" from node to node. The same two cases of false alarm rate are considered (10 for N3 and 35 for N4) and can again be compared.

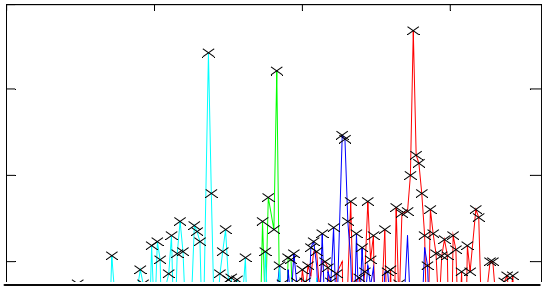

Figure 9. Target contacts for cases N5 and N6, with the target being "handed off" from one node to the next.

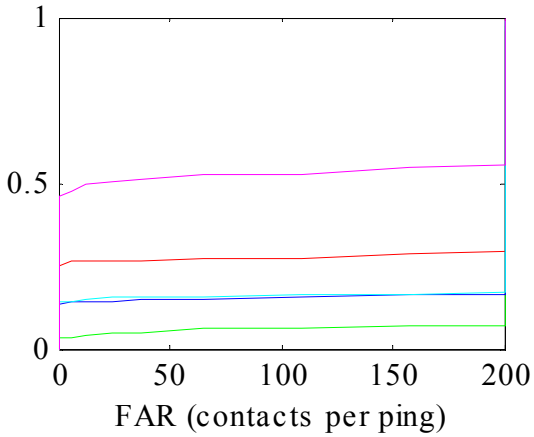

Fig. 10. Individual and fused (cyan) ROC curve performance for cases N5 and N6.

Scenario N7 can be realized by applying slightly different detection thresholds to each detection node. This will produce different average per ping false alarm rates (0, 5, 10, and 35). The target detection contacts have high PD as shown previously in figure 5 (for cases N1 and N2). The issue for this case is how that tracker can cope with differing false alarm rates on various nodes. This case may be encountered when there are different system capabilities or environmental views that produce different clutter rates.

Case N8 is achieved by subtracting 14dB from all the target contacts in the data set. The detections that pass the threshold are shown in figure 11. Here we assume a low, constant false alarm of 10 per source-receiver ping amongst the nodes in the multistatic network. Here the challenge is that there will be very few target contacts from which to make temporal associations. This is an example of a hyper-spaced surveillance field, and it may require different data fusion and tracking approaches.

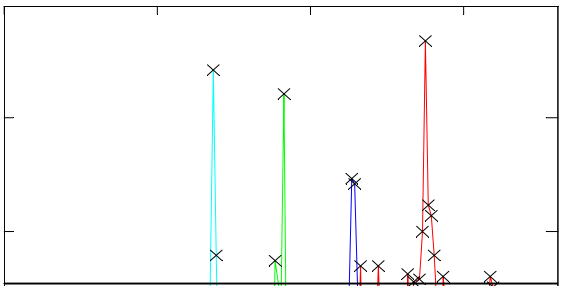

Figure 11. Target contacts for case N8 with the multistatic system losing contact nodes.

7 Contact Localization

Statistically significant measurement covariance matrices are required for effective target tracking. Our contact data simulation allows for the computation of (range, bearing) measurements from the receiver, along with a measurement covariance that reflects assumptions about errors in the following measured quantities: source and receiver locations, array heading, speed of sound, and contact timing and bearing information. Details of this analysis are in [3].

There is good agreement between the analytical measurement covariance expressions and the actual distribution of localization errors. Figure 12 illustrates that, for relatively large measurement errors, there is less agreement due to the small-error approximations on which the analysis is based.

As an example, consider sources at (1000, 100) and (-1000, 2000), a common receiver at (-1000, 1000), and the error statistics $\sigma_\tau = 0.01$ sec (timing), $\sigma_\theta = 1$ deg (bearing), and $\sigma_{\phi^R} = 1$ deg (array heading). In Figure 13, we illustrate the multistatic localization error with combined bistatic measurements (log of trace is plotted). It is significant to note that there is no singularity region for multistatic localization error, unless all bistatic pairs share a singularity region (i.e. common lines between sources and receiver).

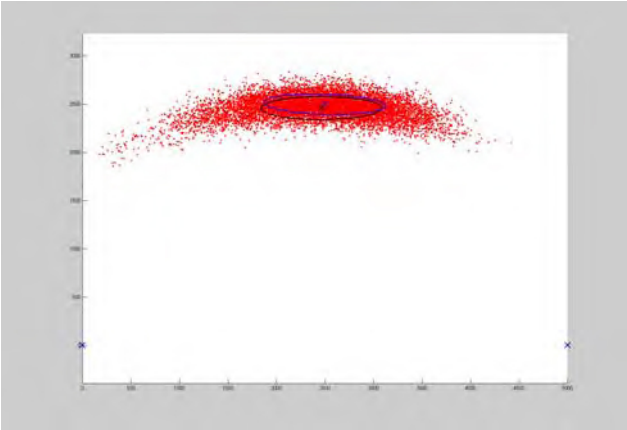

Fig. 12. Distribution of contacts with large bearing errors ($\sigma_\theta = 5\,\text{deg}$).

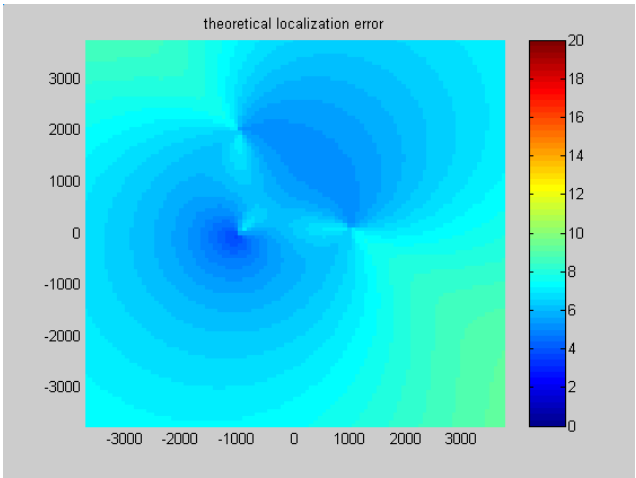

Fig. 13. Multistatic localization error.

8 Conclusions

NURC has developed a modeling and simulation methodology that can produce contact-level data sets for input to multistatic data fusion and tracking algorithms. Although the modeling capability cannot be considered high fidelity or predictive due to its simplifying assumptions, it is sufficient for creating a range of scenario types useful for tracker algorithm evaluation.

The modeling treats target-fading conditions according to the sonar equation and includes target fluctuations and Raleigh distributed noise fields. Generated contacts include localization errors, which are due to the various system measurement errors.

From a single simulated scenario, other scenario variants can easily be obtained through simple adjustments to the (tagged) target contact levels and the adjustment of the detection threshold. This simulated data set and its scenario variations have been provided to the MSTWG for its work in tracker evaluation.

In the future, the modeling approach could be extended to include Doppler waveforms, and noise-limited conditions. In addition, more sophisticated modeling of reverberation clutter could be considered.

9 References

[1] S. Coraluppi, D. Grimmett, and P. de Theije, Benchmark Evaluation of Multistatic Sonar Trackers, in *Proceedings of the 9th International Conference on Information Fusion*, July 2006, Florence, Italy.

[2] D. Grimmett, Multistatic Sensor Placement with the Complimentary use of Doppler Sensitive and Insensitive Waveforms, in *Proceedings of the 9th International Conference on Information Fusion*, July 2006, Florence, Italy.

[3] S. Coraluppi, Localization and Fusion in Multistatic Sonar, in *Proceedings of the 8th International Conference on Information Fusion*, July 2005, Philadelphia PA, USA.

[4] B. La Cour, C. Collins, and J. Landry, Multi-everything Sonar Simulator (MESS), in *Proceedings of the 9th International Conference on Information Fusion*, July 2006, Florence, Italy.

Intentionally blank page

Document Data Sheet

Security Classification		Project No.
RELEASABLE TO THE PUBLIC		
Document Serial No.	**Date of Issue**	**Total Pages**
NURC-PR-2006-008	August 2006	11 pp.

Author(s)

Grimmett Douglas, Coraluppi Stefano

Title

Contact-Level Multistatic Sonar Data Simulator for Tracker Performance

Abstract

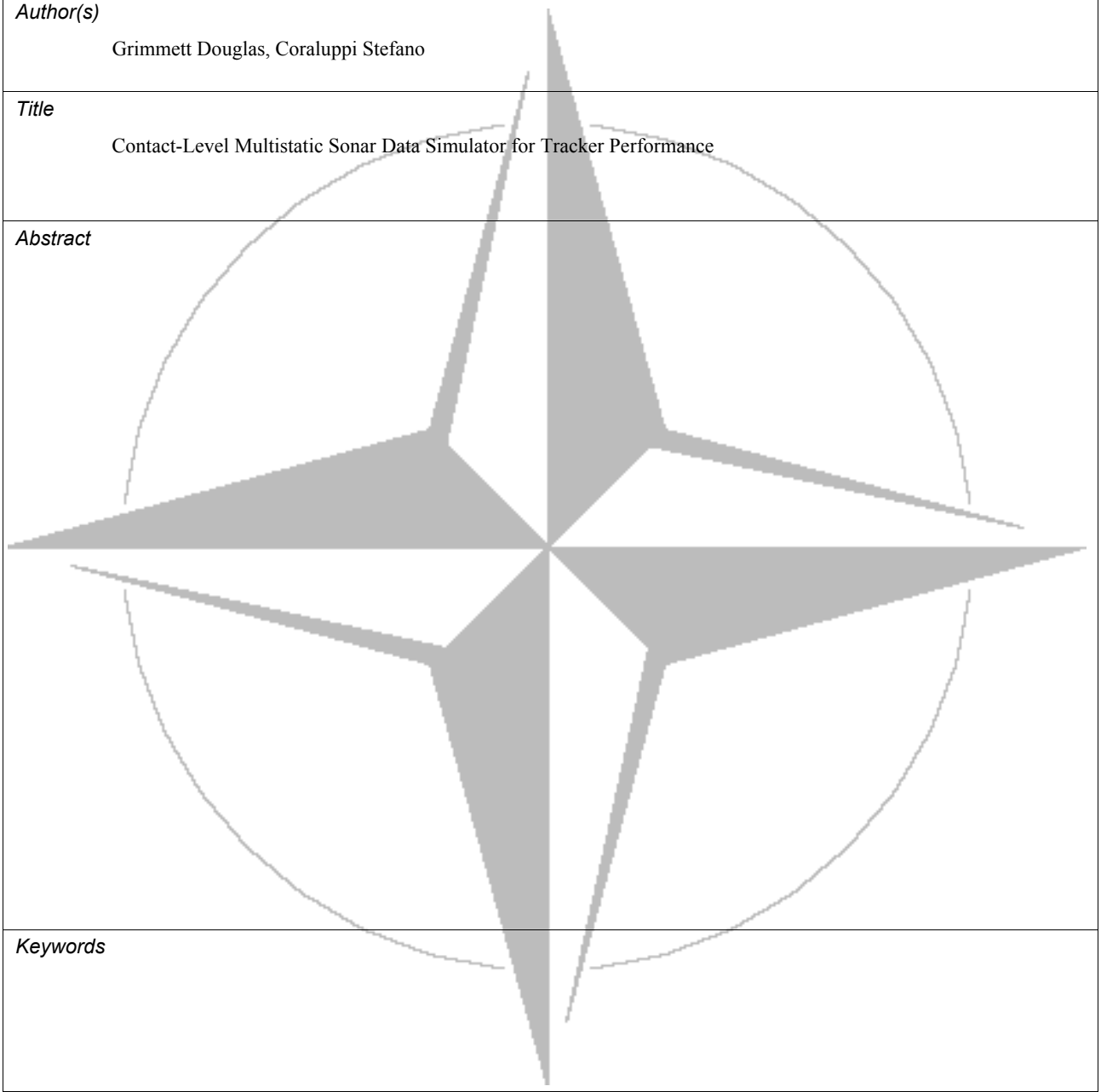

Keywords

Issuing Organization

NATO Undersea Research Centre
Viale San Bartolomeo 400, 19138 La Spezia, Italy

[From N. America:
NATO Undersea Research Centre
(New York) APO AE 09613-5000]

Tel: +39 0187 527 361
Fax:+39 0187 527 700

E-mail: library@nurc.nato.int